Sol-immobilized vs deposited-precipitated Au nanoparticles supported on CeO2 for furfural oxidative esterification

Title: Sol-immobilized vs deposited-precipitated Au nanoparticles supported on CeO_2 for furfural oxidative esterification

Short title: Au nanoparticles on CeO_2 for furfural oxidative esterification

Federica Menegazzo[a], Michela Signoretto[a*], Tania Fantinel,[a] Maela Manzoli[b]

[a.] Department of Molecular Sciences and Nanosystems, Ca' Foscari University Venice and INSTM-RU Ve, Via Torino 155, 30172 Venezia Mestre, Italy

*corresponding author: miky@unive.it

[b.] Department of Drug Science and Technology and NIS - Centre for Nanostructured Interfaces and Surfaces, University of Turin, Via P. Giuria 9, 10125 Turin, Italy

Abstract

BACKGROUND: The nonedible nature of lignocellulose makes this an important raw material for future biorefineries. The work concerns the oxidative esterification of furfural (a C5 compound) to alkyl furoate, which find applications in the fine chemical industry.

RESULTS: Very efficient Au/CeO_2 catalysts for furfural oxidative esterification were prepared by deposition of gold colloids using polyvinyl alcohol as protective agent. The catalysts showed complete conversion and selectivity without the presence of a base. Sol-immobilized catalysts displayed better catalytic performances than Au/CeO_2 prepared by deposition-precipitation (74% conversion). It was proposed that polyvinyl alcohol molecules act not only as gold stabilizer, but they leave the ceria support to be more free and available for catalysis. The reaction is extremely sensitive to the temperature, but it can be carried out at very low pressures. Sol-immobilized catalysts do not require any preliminary calcination to be activated and can be recovered by simple filtration: no oxidation of the exhausted catalyst is required for at least 6 catalytic runs.

CONCLUSION The new catalyst is active, selective, recyclable and proper for an industrial chemistry based on renewable resources. The furoate ester can be obtained with optimal yields by a process greener than the actual one.

Keywords: gold catalyst; CeO_2; furfural, oxidation; esterification; biomass.

Introduction

In recent years, the production of fuel and chemicals from biomass, involving the transformation of selected platform molecules, has received much attention, due to the possibility to replace the products coming from petrolchemistry. Biomass valorisation in the framework of biorefineries has enormous production potential. Furfural (2-FA), coming from the dehydration of C5 biomass sugars, has a very high platform prospective for chemical production in biorefineries. However, the successfully replacing petroleum-based fuels and chemicals with lignocellulose biomass-based products will require high-yield, low-cost and energetically efficient targeted upgrading processes. Oxidation is a key reaction in organic synthesis and it will likely play a significant role in the development of value-added chemicals from biomass. For example, oxidation of furfural can allow production of relevant carboxylic acids, such as furoic and maleic acids.[1]

According to Scheme 1, the furfural molecule can be converted into methyl-2-furoate by furfural oxidative esterification:

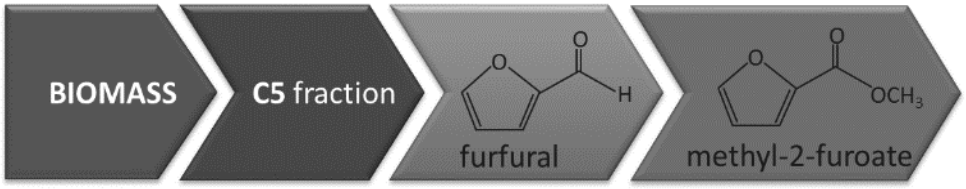

Scheme 1: Methyl-2-furoate obtained by 2-FA coming from the C5 fraction of biomass.

Methyl-2-furoate is employed as flavour and fragrance component and is a higher added value product. In this frame, the formulation of new heterogeneous catalysts which are able to work in the presence of molecular oxygen can represent a green alternative to traditional, toxic chemical oxidants to convert 2-FA into methyl-2-furoate. Traditionally, the ester is prepared by oxidizing furfural with potassium permanganate, preferably using acetone as solvent, and reacting the furoic acid so formed with methyl or ethyl alcohol, in the presence

of sulphuric acid. These substances have a substantial negative impact on the environment and a sustainable alternative would be to avoid their use.

Furfural oxidative esterification has been investigated firstly by Christensen *et al.*[2] using a commercial Au/TiO_2 catalyst by the World Gold Council in the presence of a base (8% CH_3ONa). In contrast, Corma *et al.* studied the same reaction using gold-based catalysts, without using a base, which would make the process less green and less advantageous from an economic point of view.[3] Gold-based catalysts on different supports have been extensively investigated for a base free esterification of furfural.[4-7] The characterisation results demonstrated that, differently from Au/ZrO_2 catalysts[4, 5], Au/CeO_2 catalysts need no gold cluster to activate oxygen and to catalyse the reaction.[8] Therefore, the design of new catalysts containing gold nanoparticles with opportune modulated size is a key step for the optimization of oxidative esterification reactions.

The immobilization of pre-formed metallic sols is widely applied. The method is based on the preparation of Au nanoparticles and their subsequent immobilization on a support. The advantage of using this technique principally lies in its applicability regardless of the type of support employed and the possible control on particle size/distribution, obtaining normally highly dispersed metal catalysts.[9] Indeed, the use of metallic sols has been proposed to tailor the size of the supported gold particle[10]. Gold colloids have been known since ancient times, but for catalytic purposes the gold particle diameter has to be <10 nm.[11] The reduction of chloroauric solution with tetrakis(hydroxymethyl)phosphonium chloride (THPC)/NaOH system[12] or sodium borohydride in the presence of protective molecules[13, 14], is a suitable procedure as a smaller particle with a narrower distribution is obtained. Polymers, such as polyvinyl alcohol (PVA) are commercially available, relatively inexpensive, well water-soluble, non-toxic, and very effective stabilizers for colloid preparation.[15] PVA contains a long-carbon-chain backbone with hydroxyl groups, and acts as steric stabilizer[16], coordinating to gold by van der Waals interactions.

Cerium oxide received a great deal of interest from researchers because of its unusual properties, including high chemical stability, high charge transfer capability, non-toxicity oxygen ion conductivity, biocompatibility[17] and "oxygen storage capacity" (OSC).[18] The aptitude to change oxidation state is related to its ability to store and release oxygen, a property that make CeO_2 a very interesting support for oxidation reactions.[19]

Following the ongoing program to design new Au-based catalytic systems for ~~the~~ environmentally benign transformations of furfural into valuable chemicals, we have herein investigated the effect of the sol immobilization synthesis to prepare Au/CeO_2 (Ausol) catalysts by deposition of gold colloids.

Polyvinyl alcohol was used as protective agent. These catalysts have been tested in the furfural oxidative esterification and the results have been compared to those obtained for an Au/CeO_2 catalyst in which gold has been introduced by classical deposition precipitation. It was found that the Ausol catalyst showed the best catalytic activity if previously submitted to calcination at 500°C.

Therefore, the goal of the present work is to synthesize an active and easily recyclable Au/CeO_2 catalytic system for furfural oxidative esterification. The catalyst should be able to operate without the presence of a base, which negatively affects the sustainability of the process.

Experimental

Synthesis of the support

Ceria support was synthesized by precipitation from $(NH_4)_2Ce(NO_3)_6$ by urea in aqueous solution.[20, 21] The solution was stirred and boiled at 100 °C for 6 h, the precipitate was washed twice in boiling deionized water and dried at 110 °C for 20 hours and then calcined at 500 °C in flowing air (50 mL/min) for 3 hours.

Preparation of the catalysts by sol immobilization method

A 1 wt.% polyvinyl alcohol (PVA) solution was added to an aqueous $HAuCl_4$ solution under vigorous stirring at 0 °C (PVA/Au (w/w)= 0.5). Then a freshly prepared 0.1 M solution of $NaBH_4$ ($NaBH_4$/Au (mol/mol)= 4) was added, to form a ruby-red metallic sol. Within 5 minutes of sol generation, the sol was immobilized by adding the ceria support (Ce500) under vigorous stirring and aged for 12 hours at 0 °C. The amount of support was calculated as having a final gold loading of 1.5 wt %. After filtration, the sample was washed with distilled water (5 times with 100 mL). The sample was dried at 110 °C for 20 hours (Ausol). Part of the material was finally calcined in flowing air (30 mL/min) for 1 hour at 300 °C (Ausol300) or 500 °C (Ausol500).

Preparation of the catalyst by gold deposition-precipitation (dp)

1.5 wt% of gold was added by deposition-precipitation (dp) at pH=8.6: the support was suspended in an aqueous solution of $HAuCl_4 \cdot 3H_2O$ for 3 hours and the pH was controlled by the addition of NaOH (0,5 M). After filtration the sample was washed with distilled water (5 times with 100 mL), dried at 35 °C for 20 hours and finally calcined in flowing air (30 mL/min) at 500 °C for 1 hour. The obtained sample will be hereafter denoted as Audp500.

Catalytic activity measurements

2-FA oxidative esterification with oxygen and methanol was investigated at 120 °C, without $NaCH_3O$ addition, using a mechanical stirred autoclave fitted with an external jacket.[6] Catalyst (100 mg), 2-FA (Sigma Aldrich, ›99%; 300 μL) and n-octane (Sigma Aldrich, ›99%; 150 μL), used as internal standard, were added to the methanol solvent (150 mL). The reactor was charged with oxygen (typically 6 bar) and stirred at 1000 rpm. The progress of the reaction was determined by gas-chromatographic analysis of the converted mixture (capillary column HP-5, FID detector). Preliminary experiments showed that the system

works in a strictly kinetic regime.[5] Moreover, it was previously checked that ~~the~~ bare ceria is not active under the reaction conditions used in this work. [8]

Recyclability tests were performed on the catalyst after completion of the reaction. The catalyst was filtered, washed with the solvent, dried and charged again for consecutive reaction runs. This process was repeated for 6 runs.

Methods

The gold amount for both fresh and exhausted catalysts was determined by atomic absorption spectroscopy (AAS) after microwave digestion of the samples (100 mg) in *aqua regia* using a Perkin-Elmer Analyst 100.

Thermal analyses (TG/DTA) were performed on a NETZSCH STA 409 PC/PG instrument in flowing air (20 mL/min) with temperature rate set at 5 °C/min in the 25-900 °C temperature range.

Temperature programmed oxidation (TPO) measurements were carried out to determine the substances released during the TG/DTA thermal treatment, in a lab made equipment: samples (100 mg) were heated with a temperature rate of 10 °C/min from 25 °C to 900 °C in air (40 mL/min). The effluent gases were analysed by a Genesys 422 quadrupole mass analyser (QMS). The signals for masses 18, 28, 44, 48, 64 were recorded.

Diffuse reflectance UV-Vis-NIR analysis was performed on the samples in the form of powders. The as prepared samples were placed in a quartz cell, allowing treatments in controlled atmosphere and temperature, but spectra recording only at room temperature (r.t.). Diffuse reflectance UV-Vis-NIR spectra were collected at r.t. on a Varian Cary 5000 spectrophotometer, working in the range of wavenumbers 50000-4000 cm^{-1}. UV-Vis-NIR spectra are reported in the Kubelka-Munk function [$f(R\infty)=(1-R\infty)2/2R\infty$; $R\infty$=reflectance of an “infinitely thick” layer of the sample].

High resolution transmission microscopy (HRTEM) measurements were performed using a side entry Jeol JEM 3010 (300 kV) microscope equipped with a LaB_6 filament and fitted with X-ray EDS analysis by a Link ISIS 200 detector. For analyses, the powdered samples were deposited on a copper grid, coated with a porous carbon film. All digital micrographs were acquired by an Ultrascan 1000 camera and the images were processed by Gatan digital micrograph. A statistical evaluation of the Au particle size was performed for each sample. Histograms of the particle size distribution were obtained by considering at least 200 particles on the TEM and HRTEM images, and the mean particle diameter (d_m) was calculated as $d_m = \Sigma d_i n_i / \Sigma n_i$, where n_i was the number of particles of diameter di. The counting was carried out on electron micrographs acquired starting from 150,000 magnification, at which the poor contrast phase between Au and CeO_2 appears minimised and favours clear observation of the metal nanoparticles.

Results and discussion

Catalytic activity results

The catalytic activity displayed by the sample prepared by sol-immobilization method was compared with that obtained for the catalyst prepared by the deposition-precipitation procedure. In particular, the Audp500 catalyst was chosen as a reference since we have previously demonstrated[8] that it is the best performing catalyst for this reaction. Table 1 reports the activity results for the new samples and the Au average size of the catalysts. A total selectivity to methyl-2-furoate has been observed for all catalysts in the same reaction conditions. However, the samples synthesized by sol immobilization method display better conversion than Audp500. Actually, despite a good dispersion, the Audp500 sample shows the lowest conversion. These findings demonstrated that the preparation method employed to immobilize gold on the same support affects the catalytic performances. More in detail, ~~a together~~ a complete conversion with total selectivity were observed after 90 minutes of

reaction in the case of Ausol, Ausol300 and Ausol500 samples (Table 1). These results indicate that the final calcination temperature to which the samples underwent (500 °C) did not affect the catalytic performances under standard conditions (120 °C - 6 bar O_2).

This is completely different from what normally observed for gold catalysts prepared by dp.[4, 5, 8] For example, under the same reaction conditions, the sample prepared by dp and calcined at 300 °C showed modest conversion (54 %) under the same reaction conditions.[8]

These results are of paramount importance because they indicate that the catalysts prepared by sol-immobilization do not require any preliminary calcination to be activated, resulting in a remarkable advantage for the optimization of the catalyst design as well as for the overall process from an economic point of view. Moreover, if compared to the results related to Audp500, a beneficial effect of the sol-immobilization preparation method on the stabilization of the Au nanoparticles up to 500 °C could be deduced.

Characterization of the catalysts

In order to highlight the parameters ruling the very good catalytic performances displayed by the catalysts prepared by sol immobilization method and to establish structure-activity relationships, the samples have been thoroughly characterised. Audp500 catalyst was also studied for comparison purposes, to stress on the influence of the preparation method.

All the Ausol-samples have an effective gold content (1.4 wt %) which is lower than the nominal one (1.5 wt %). On the contrary, the gold effective amount of the Audp500 sample is the same as its nominal content (1.5 wt %).

Thermal TG/DTA analyses and TPO measures were carried out in order to have information on the behaviour of the samples during calcination, starting from room temperature up to 900 °C in O_2 atmosphere. In particular, we were interested in verifying if the PVA protecting agent is still present after calcination at 300 °C or at 500 °C. The results are reported in Figure 1. The TG curve (section a) indicates that the Ausol sample underwent to

a 5 wt% weight loss between 50 °C and 350 °C. Such weight loss is associated to an endothermic peak in the DTA curve, due to the release of water from the surface of the ceria support, as well as to a large exothermic band centred at 200 °C (section b). The latter peak can be rationally ascribed to carbonate compounds since it is well known that ceria is inclined to absorb CO_2 from atmosphere. Then the TG profile decreases of about 2 wt% until 450 °C and at the same time the DTA curve shows an exothermic band, that is reasonably due to the presence of the PVA surfactant on the material. As regard as the TPO measurements, the profiles of Ausol and Ausol300 (section c) display the evolution of CO_2 between 50 °C and 350 °C and at 450 °C. On the contrary, the peak at 450 °C is almost negligible in the case of Ausol500. Therefore, the calcination at 300 °C allows the partial recovering of PVA, whilst the calcination at 500°C leads to almost complete decomposition of PVA.

To more deeply investigate the nature of the gold species present on the different samples, diffuse reflectance UV-Vis-NIR (DRUV-Vis-NIR) measurements were carried out and the spectra of the as prepared samples in the 50000-4000 cm^{-1} range are reported in Figure 2. First of all, being all catalysts supported on the same material, absorption bands at about 42500, 36000 and 29000 cm^{-1} due to $Ce^{3+} \leftarrow O_2^-$ charge transfer[22-25], to the electron transitions from the valence band to the conduction band (O(2p) to Ce (4f) and to interband transitions, respectively have been detected. However, the absorptions related to $Ce^{3+} \leftarrow O_2^-$ and $Ce^{4+} \leftarrow O_2^-$ transitions have different relative intensity depending on the nature of sample: in particular, the higher is the intensity of the former absorption the lower is the intensity of the latter one. These features indicate that upon calcination at 300°C and 500°C, Ce^{3+} vacancies are depleted forming Ce^{4+} on Ausol300 (grey curve) and Ausol500 (bold curve). Moreover, the trend observed as for the component at 42500 cm^{-1}, assigned to $Ce^{3+} \leftarrow O_2^-$ charge transfer, can be taken as a qualitative indication that the Audp500 catalyst

(dashed curve) is containing the highest amount of ceria defects, suggesting that the preparation method used to introduce gold influenced someway the ceria support.

The typical plasmonic absorption, due to the presence of gold nanoparticles[26-29], has been detected in all cases in the 22000-10000 cm^{-1} region (Figure 2, inset). Moreover, both position and shape of the maxima related to Ausol (fine curve), Ausol300 (grey curve) and Ausol500 (bold curve) are very similar and an increase in intensity is observed when increasing the calcination temperature to which the samples underwent, i.e. passing from room temperature up to 300 °C and 500 °C. This effect is more evident in the case of Ausol500 (bold curve), that shows the most intense plasmonic absorption at 18600 cm^{-1}, indicating that some agglomeration of the gold nanoparticles occurred upon calcination at 500°C. However, basing on DRUV-Vis-NIR findings, this effect is restrained, indicating that the PVA molecules effectively behave as protecting agent by stabilizing the gold nanoparticles up to 500 °C, as proposed in paragraph 3.1.

The plasmonic band related to Audp500 (dashed curve) is red shifted in position at about 17600 cm^{-1}, shows the highest intensity and its shape is broader than that related to the samples prepared by sol-immobilization. Such spectroscopic features revealed that some contribution to the absorption by Au nanoparticles with larger size occurred and that the size distribution of the Au nanoparticles present on the dp catalyst is rather heterogeneous. Moreover, the presence of flat highly dispersed Au clusters, flattened on the support due to the strong interaction with the defects cannot be excluded. These species can exhibit both transverse and longitudinal plasmons.[30-32] Irregular plate-like gold nanoparticles were observed on Au/ZrO_2 samples prepared by deposition-precipitation.[33] These morphologies were responsible for the plasmonic contribution at high wavelengths.[33] DRUV-Vis-NIR analysis put in evidence a role on the gold size by the final calcination to which the catalysts were submitted[8], as well as an effect of the preparation method. The sol-immobilization procedure, due to the PVA protecting agent, guarantees higher stabilization of the Au

nanoparticles resulting in a more homogeneous gold dispersion if compared to the deposition-precipitation method. In the case of Audp500, the metal-support interaction is not mediated by the PVA molecules, giving rise to the presence of gold species heterogeneously dispersed as for size and shape.

DRUV-Vis-NIR results showed that the calcination temperature affected on one hand, the final size of the PVA-protected Au particles and, on the other hand, it gave rise to less defective ceria. This observation is consistent with the observed decrease in intensity of the absorption related to $Ce^{3+} \leftarrow O_2^-$ transition accompanied by the simultaneous increase in intensity of the component related to the $Ce^{4+} \leftarrow O_2^-$ transition after calcination. Moreover, the catalytic activity measurements revealed that complete (>99 %) selectivity and conversion were achieved, independently from the Au size.

HRTEM analyses were performed on the Ausol and Ausol500 catalysts to have information on the overall morphology as well as on the Au particle size. The results were compared with those obtained for Audp500 in order to put in evidence particular features eventually arisen from the different preparation method with which gold has been inserted, given the same support. All these data are summarized in Figure 3. All catalysts are supported on cubic CeO_2, mainly exposing the (111) face together with the (200) and (220) faces (JCPDS file number 34-394). However, the diffraction fringes corresponding to the (200) face of the monoclinic Ce_6O_{11} phase have also been observed in the case of Ausol (JCPDS file number 32-196). The presence of crystalline planes related to a ceria defective phase is in agreement with what observed by DR UV-Vis spectroscopy and proposed. In addition, the Ausol catalyst contains rounded gold nanoparticles (section a) with average diameter equal to 3.0 ± 1.7 nm (section d).

The particle size distribution indicates that the majority of the gold species has size around 2.5 nm. An agglomeration of the gold nanoparticles with size 2.5 nm into bigger particles with size mainly around 5 nm occurred in the case of Ausol500 (section b). Indeed, the Au

average size is 4.7 ± 0.8 nm (section e) and such increase with respect to Ausol is due to the calcination at 500°C. On the contrary, gold nanoparticles with more heterogeneous size have been observed on Audp500 (section c), as indicated by the broader particle size distribution (section f). Small gold particles with average size 3.4 ± 1.3 nm as well as big agglomerates with size around 25 nm have been observed. The latter species can also explain the presence of the component at higher wavelengths in the DRUV-Vis-NIR spectrum of Audp500 (see Figure 2, dashed curve). These findings are in agreement with the proposed beneficial effect of the sol-immobilization preparation method vs the deposition-precipitation procedure in the stabilization of the Au nanoparticles. However, the differences in the gold size here discussed do not seem to be enough relevant to justify the increase in the catalytic activity observed in the presence of the catalysts prepared by sol-immobilization method. In addition, Ausol, Ausol300 and Ausol500 give all complete conversion, despite having plasmonic bands somewhat differing for intensity and position, further indicating that the gold size poorly affects the furfural conversion to methylfuroate. The strength and the nature of the interaction between the protective molecule and the gold unsupported nanoparticle surface is of utmost importance. The protective layer should contribute to the colloid stability ~~to one hand~~ and in addition it should not be irreversibly adsorbed on the Au active sites of the nanoparticles providing convenient accessibility to reactant ~~on the other hand~~[34]. From a catalytic point of view, the milder is the interaction between the particle surface and the capping agent, the higher is the activity increase. However, anchoring the gold nanoparticles to the ceria support can circumvent problems of stability due to the adopted reaction conditions. In addition, despite there is no more PVA in the Ausol500 catalyst (as shown by TPO and TG-DTA analyses, Figure 1) the catalytic performances are unchanged. Therefore, the presence of PVA has no influence during batch reaction. Nevertheless, an effect related to the presence of the PVA molecules during calcination can be proposed. It is reasonable that the gold nanoparticles present on the samples prepared by PVA are already

formed and stable and they do not strongly interact with the support during calcination. On the contrary, a strong interaction between the ceria support and the gold nanoparticles is achieved during the calcination of a sample prepared by dp, resulting in a catalyst in which the surface of the ceria support is less free and therefore less available to the reactant adsorption and activation. Ceria has a crucial role in this reaction: we recently reported that Au/CeO_2 catalyst needs no gold cluster to activate oxygen and to catalyse the furfural oxidative esterification[8], due to the fact that in reaction conditions ceria is able to provide activated oxygen instead of gold clusters with simultaneous creation of neutral oxygen vacancies. In addition, the created oxygen vacancies could further play a role by activating the reactant oxygen molecules coming from the gas phase[35, 36] and therefore ~~further~~ enhance the reactivity of the Au/CeO_2 system. A strong morphological effect of gold on the reducibility and on the CO oxidation activity of ceria was established.[37] In the present study, as for the samples prepared by sol-immobilisation, all defective ceria supports play a major role in the reaction than a ceria support that is strongly interacting with gold nanoparticles.

Optimization of the process

There are many examples in the literature that stress on the paramount importance of choosing gold nanoparticles with ~~opportune~~ size advantageous for ~~the~~ oxidative esterification reactions. It has been recently reported that small molecules (CO, NO, etc.) can be activated only on small gold nanoparticles or roughened Au(111) surfaces, i.e. in the presence of considerable disorder, whereas well-ordered Au(111) single crystals or extended metal films are active in the reaction of certain large molecules[38], such as those involved in the furfural oxidative esterification reaction. However, it would be also advantageous to optimize the operating conditions in order to make the process environmentally friendly and industrially feasible. Therefore, a key step is to investigate how to find the best process

conditions, in terms of pressure and reaction time, in order to yield a green, safe, economic and sustainable process.

First, the effect of the reaction time on the oxidative esterification of furfural over the Ausol catalyst was investigated. Different catalytic tests by varying only the time of reaction have been performed (Figure 4). Selectivity is very high (>99 %) for all catalytic tests and it is constant for the time range in which it was investigated. These data indicate that the transformation of furfural into the corresponding furoate happens without any side reactions on the Ausol catalyst. On the contrary, as expected, the conversion increases with the reaction time. In particular, the conversion rises until the maximum value after 90 minutes of reaction.

The research work was then addressed to the investigation of the effect of the oxygen pressure on the 2-FA esterification reaction. Such effect was evaluated starting from 6 bar O_2 and dropping to lower values until 1 bar O_2 (relative pressure). As reported in Figure 5 (section a) the pressure effect on the conversion of furfural to methyl-2-furoate is almost negligible and, despite of the pressure lowering, it is possible to obtain always high conversions. Selectivity is constant at >99 % and it is not affected by pressure changes. Such negligible effect of the pressure on the oxidative esterification of furfural has been previously found for Au/ZrO_2 samples synthesized by dp.[7] The obtained results are quite relevant, since the reaction can be carried out at very low pressures, therefore reducing the consumption of oxidant and making more harmless the experimental setup. Moreover, looking at possible application of the process on an industrial scale, the low operating pressure would lead to a decrease in costs related to plant design.

The study of the effect of the reaction temperature on the catalytic performances during furfural esterification was performed at 60 minutes of reaction, in the presence of a 6 bar oxygen pressure and lowering the temperature from 120 °C down to 80 °C. The screening highlights a pronounced effect of the temperature on the furfural conversion (Figure 5,

section b). More in detail, a decrease of the temperature from 120 °C to 80 °C causes a drop in the conversion from 80 % to 14 %, whilst the results obtained for the selectivity are not dependent from ~~to~~ the reaction temperature. In conclusion, the catalytic performances on the Ausol sample are strictly connected to the temperature of reaction, whereas the effect of pressure is not relevant.

Reusability of the catalyst

One of the main drawbacks in the industrial exploitation of a catalyst lies in a poor stability: for commercial usage, the catalysts need to be stable and should not deteriorate with the elapse of time and with use. Therefore, the nature of the catalyst deactivation as well as the possibility of regaining the lost catalytic activity, either during the operation of the reaction or in a separate regeneration step, are important factors that determine process options.[39] The recyclability of the Ausol catalyst was studied under the optimized conditions and the desired product with a high yield of reaction was obtained after 1-6 runs (Figure 6).

In particular, after reaction completion, the catalyst was washed with the solvent, dried and stored for consecutive reaction runs. This process was repeated for 6 runs and no significant decrease of conversion was observed. Selectivity was maintained at >99 % up to the 4th cycle and then slightly decreased to 95 % during runs 5 and 6. The experimental procedure with Ausol catalyst is quite straightforward and the catalyst can be recovered by simple filtration, differently from what observed during recyclability tests carried out on gold based samples synthesized by dp[40, 5]. It was reported that the catalysts needed an intermediate thermal regeneration at 450 °C in order to completely restore the initial catalytic performances.

With regard to furfural oxidative esterification reaction, the soiling by organic species has been identified as the main cause of deactivation.[5] In particular, it was shown that the

presence of PVA located at the interface between gold nanoparticles and ~~on~~ the surface of the support can act as protecting agent.

It is widely reported that stabilizers such as PVA interact with the surface of the nanoparticles competing with reactant molecules, acting as a (partial) surface poison by blocking active sites.[41, 42] Recently Prati *et al.*[34] reported on gold nanoparticles synthesized by different protective agents: only PVA was able to efficiently stabilize the nanoparticles against coalescence and to maintain the initial particle size, even after reaction, representing a quite stable system. Keeping in mind these findings, additional thermal TG/DTA analyses were carried out on the used Ausol catalyst in order to monitor the presence of PVA after 6 runs ~~of reaction~~ and to investigate the occurrence of poisoning. The results are reported in Figure 7.

A 3 wt % drop between 300 °C and 350 °C is observed in the TG curve (Figure 5, section a) simultaneously with the appearance of an intense and narrow peak in the DTA profile in the same temperature range (section b of Figure 5). According to previous studies[5], such weight loss is ascribable to organic species remained on the material after reaction. Moreover, the band at 450 °C in the DTA profile and the corresponding drop in the TG curve reveal the presence of residue PVA on the catalyst. Therefore, the batch reaction does not lead to the complete disappearance of PVA from the surface of the catalyst.

In section a of Figure 8 an HRTEM representative image of the Ausol sample after 6 catalytic runs is reported. The Ausol used catalyst contains rounded gold nanoparticles (indicated by arrows) similar to those observed on the fresh sample (see Figure 3, section a) with average diameter equal to 4.6 ± 2.0 nm (section c). However, the comparison with the Au particle size distribution of the fresh sample (reported in section b for convenience) reveals the presence of an enhanced amount of nanoparticles with size around 5 nm, indicating that some agglomeration occurred after the six catalytic runs. However, the

HRTEM findings on the Ausol used catalyst further confirm that the interaction between the gold nanoparticles and the PVA protective agent is maintained during reaction.

Comparison with other catalytic systems prepared by dp under the same reaction conditions

In order to further reveal the merit of sol-immobilized technology generated Au/CeO_2 catalyst for the oxidative esterification reaction, the catalytic performances displayed by the Ausol catalyst were compared with those observed for several Au catalysts prepared by dp under the same reaction conditions (reaction at 120 °C - 6 bar O_2 – 90 min of reaction).

Table 2 summarises the catalytic performances in the 2-FA oxidative esterification for an extended series of previously investigated samples synthesized by dp. A closer inspection of the results reveals that to obtain catalytically effective materials, it is important not only to control the Au particle size, but also to focus on the nature of the support as well as on the synthetic parameters (i.e. calcination temperature). In particular, it can be inferred that both conversion and selectivity observed for the Ausol catalyst are as good as those related to the most performing dp catalysts, confirming that the sol-immobilisation procedure is suitable for obtaining active gold catalysts. However, it is worth noting that the experimental procedure with Ausol catalyst is quite straightforward and the catalyst can be recovered by simple filtration. This is very important, because the samples synthesized by dp need to be thermally regenerated (O_2, 450 °C) to regain the starting catalytic properties[40, 5]. These advantages can be reasonably attributed to the presence of PVA on the surface of the catalyst. Indeed, the principal causes of catalyst deactivation are well recognized, namely: metal sintering, metal leaching, fouling of the active sites.

Conclusions

Very efficient Au/CeO_2 catalysts for the oxidative esterification of furfural were prepared by deposition of gold colloids using polyvinyl alcohol as protective agent. The catalysts showed

high conversion and complete selectivity even at short reaction times without the presence of a base, which negatively affects the sustainability of the process. The results were compared to those obtained for an Au/CeO_2 catalyst prepared by classical deposition precipitation and a positive effect of the presence of the PVA molecules was pointed out. In particular, it was shown that polyvinyl alcohol behaves as stabilizer of gold.

The effect of reaction time, reaction temperature and oxygen pressure were also investigated in view of an optimization of the process. It was found that the furfural conversion into methyl-2-furoate happens without any side reactions on the Ausol catalyst. The effect of oxygen pressure on the furfural esterification is almost negligible and high conversions are always obtained even at low pressures. Selectivity is constant at values >99 % and it is not affected by pressure changes. Therefore, the catalytic data indicated that the reaction can be carried out at very low pressures, resulting in a drop of the consumption of oxidant. Moreover, the experimental setup would be more harmless and the low operating pressure would lead to a decrease in costs related to plant design. However, the catalytic performances are strictly connected to the reaction temperature.

Another very important point is the stability and reusability of the catalyst. The calcination temperature at 300 °C or at 500 °C does not significantly affect the final size of the PVA-protected Au particles. Moreover, complete conversion and selectivity were observed, given the same Au size, indicating that the Ausol catalysts prepared by sol-immobilization do not require any preliminary calcination to be activated. This finding represents a remarkable advantage for the optimization of the catalyst design as well as for the overall process from an economic point of view.

The Ausol catalyst can be recovered by simple filtration and no oxidation of the exhausted catalyst is required for at least 6 catalytic runs. The catalyst was simply washed with the solvent, dried and stored for consecutive reaction run after reaction completion.

The catalyst prepared by sol-immobilization is therefore extremely active, selective, stable and reusable. These features make the system proper for an industrial chemistry based on renewable resources.

Conflict of Interest. The authors declare that they have no conflict of interest.

Compliance with ethical standards. This article does not contain any studies with human participants or animals performed by any of the authors.

References

1 Serrano-Ruiz J C, Luque R, Clark J H, in *The role of catalysis for the sustainable production of bio-fuels and bio-chemical*, ed by Triantafyllidis K, Lappas A., Stocker M, Elsevier, Amsterdam, pp 557-576 (2013).

2 E Taarning, IS Nielsen, K Egeblad, R Madsen, CH Christensen, Chemicals from renewables: aerobic oxidation of furfural and hydroxymethylfurfural over gold catalysts. *ChemSusChem*, ,**1**: 75- 78 (2008).

3 O Casanova, S Iborra, A Corma, Biomass into chemicals: One pot-base free oxidative esterification of 5-hydroxymethyl-2-furfural into 2,5-dimethylfuroate with gold on nanoparticulated ceria. *J. Catal.*, **265**: 109- 116 (2009).

4 F Pinna, A Olivo, V Trevisan, F Menegazzo, M Signoretto, M Manzoli, F Boccuzzi, The effects of gold nanosize for the exploitation of furfural by selective oxidation. *Catal. Today*, **203**: 196- 201 (2013).

5 M Signoretto, F Menegazzo, L Contessotto, F Pinna, M Manzoli, F Boccuzzi, Au/ZrO_2: an efficient and reusable catalyst for the oxidative esterification of renewable furfural. *Appl. Catal. B.*, **129**: 287- 293(2013).

6 F Menegazzo, M Signoretto, F Pinna, M Manzoli, V Aina, G Cerrato, F Boccuzzi, Oxidative esterification of renewable furfural on gold-based catalysts: Which is the best support? *J. Catal.*, **309**: 241-247 (2014).

7 F Menegazzo, T Fantinel, M Signoretto, F Pinna, M Manzoli, On the process for furfural and HMF oxidative esterification over Au/ZrO_2. *J. Catal.*, **319**: 61-70 (2014).

8 M Manzoli, F Menegazzo, M Signoretto, G Cruciani, F Pinna, Effects of synthetic parameters on the catalytic performance of Au/CeO_2 for furfural oxidative esterification. *J. Catal.*, **330**: 465-473 (2015).

9 L Prati, A Villa, The art of Manufactoring gold catalysts. *Catalysts*, **2**: 24-37 (2012).

10 JD Grunwaldt, C Kiener, C Wögerbauer, A Baiker, Preparation of Supported Gold Catalysts for Low-Temperature CO Oxidation via “Size-Controlled” Gold Colloid. *J. Catal.*, **181**: 223-232 (1991).

11 M Haruta, Size- and support-dependency in the catalysis of gold. *Catal. Today,* **36**: 153-166 (1997).

12 DG Duff, A Baiker, P Edwards, A new hydrosol of gold clusters. *Chem. Commun.* 96-98 (1993).

13 H Hirai, Y Nakao, N Toshima, Preparation of Colloidal Transition Metals in Polymers by Reduction with Alcohols or Ethers. *J. Macromol. Sci. Chem. A,* , **13**: 727-750 (1979).

14 RG Scipio, Preparation of colloidal gold particles of various sizes using sodium borohydride and sodium cyanoborohydride. *Anal. Biochem.*, **236**: 168-170 (1996).

15 Y Zhao, JA Baeza, N Koteswara Rao, L Calvo, MA Gilarranz, YD Li, L Lefferts, Unsupported PVA- and PVP-stabilized Pd nanoparticles as catalyst for nitrite hydrogenation in aqueous phase. *J. Catal.,* **318**: 162-169 (2014).

16 L Prati, G Martra, New gold catalysts for liquid phase oxidation. *Gold Bull.,* **32:** 96-101 (1999).

17 P Dutta, S Pal, M S Seehra, Y Shi, E M Eyring, R D Ernst, Concentration of Ce^{3+} and Oxygen Vacancies in Cerium Oxide Nanoparticles. *Chem Mater,* **18 (21):** 5144-5146 (2006).

18 M Melchionna, P Fornasiero, The role of ceria-based nanostructured materials in energy applications. *Materials Today*, **17**: 349-357 (2014).

19 Trovarelli A, in *Catalysis by ceria and related material*, ed by Trovarelli A, Imperial College Press, London, pp 15-50 (2002).

20 L Kundakovic, M Flytzani-Stephanopoulos, Cu- and Ag-Modified Cerium Oxide Catalysts for Methane Oxidation. *J. Catal.*, **179**: 203-221 (1998).

21 F Menegazzo, P Burti, M Signoretto, M Manzoli, S Vankova, F Boccuzzi, F Pinna, G Strukul, Effect of the addition of Au in zirconia and ceria supported Pd Catalysts for the direct synthesis of Hydrogen Peroxide. *J. Catal.,* **257**: 369-381 (2008).

22 ZC Orel, B Orel, Optical properties of pure CeO_2 and mixed CeO_2/SnO_2 thin film coatings. *Phys. Status Solidi B,* **186**: K33(1994).

23 H Kangar, H Ghazavi, M Darroudi, Size-controlled and bio-directed synthesis of ceria nanopowders and their in vitro cytotoxicity effects. *Ceramics International*, **41**: 4123-4128 (2015).

24 MI Zaki, GAM Hussein, SAA Mansour, HM Ismail, GAH Mekhemer, Ceria on silica and alumina catalysts: dispersion and surface acid-base properties as probed by X-ray diffractometry, UV-Vis diffuse reflectance and in situ IR absorption studies. *Colloids Surfaces A: Physicochem. Eng. Aspects*, **127**: 47-56 (1997).

25 MA Centeno, M Paulis, M Montes, JA Odriozola, Catalytic combustion of volatile organic compounds on Au/CeO2/Al2O3 and Au/Al2O3 catalysts. *Appl. Catal. A,* **234**: 65-78 (2002).

26 E Kowalska, OO Prieto Mahaney, R Abe, B Ohtani, Visible-light-induced photocatalysis through surface plasmon excitation of gold on titania surfaces. *Phys. Chem. Chem. Phys.,* **12**: 2344-2355 (2010).

27 J Tiggesbaumker, L Koller, HO Lutz, KH Meiwes-Broer, Giant resonances in silver-cluster photofragmentation. *Chem. Phys. Lett.,* **190**: 42-47(1992).

28 A Leibsch, Surface-plasmon dispersion and size dependence of Mie resonance: Silver versus simple metals. *Phys. Rev. B: Condens. Matter*, **48**: 11317-11328(1993).

29 A Moores, F Goettmann, The plasmon band in noble metal nanoparticles: an introduction to theory and applications. *New J. Chem.,* **30**: 1121-1132 (2006).

30 J Zhu, L Huang, J Zhao, Y Wang, Y Zhao, L Hao, Y Lu, Shape dependent resonance light scattering properties of gold nanorods. *Mater. Sci. Eng. B,* **121**: 199-203 (2005).

31 JE Park, T Momma, T Osaka, Spectroelectrochemical phenomena on surface plasmon resonance of Au nanoparticles immobilized on transparent electrode. *Electrochim. Acta,* **52**: 5914- 5923 *(*2007).

32 E Hao, RC Bailey, GC Schatz, JT Hupp, S Li, Synthesis and Optical Properties of "Branched" Gold Nanocrystals. *Nano Lett.*, **4**: 327-330 (2004).

33 F Menegazzo, M Signoretto, D Marchese, F Pinna, M Manzoli, Structure–activity relationships of Au/ZrO2 catalysts for 5-hydroxymethylfurfural oxidative esterification: Effects of zirconia sulphation on gold dispersion, position and shape. *J. Catal.*, **326**: 1-8 (2015).

34 L Prati, A Villa, Gold Colloids: From Quasi-Homogeneous to Heterogeneous Catalytic Systems. *Accounts of Chemical Research*, **47**: 855- 863 (2014).

35 VV Pushkarev, VI Kovalchuk, JL d'Itri, Probing Defect Sites on the CeO_2 Surface with Dioxygen. *J. Phys. Chem. B,* **108**: 5341- 5348 (2004).

36 F Vindigni, M Manzoli, A Damin, T Tabakova, A Zecchina, Surface and Inner Defects in Au/CeO_2 WGS Catalysts: Relation between Raman Properties, Reactivity and Morphology. *Chem. Eur. J.*, **17**: 4356- 4361 (2011).

37 J Wang, H Tan, S Yu, K Zhou, Morphological Effects of Gold Clusters on the Reactivity of Ceria Surface Oxygen. *ACS Catalysis,* **5**: 2873- 2881 (2015).

38 L Guczi, A Beck, Z Pászti, Gold catalysis: Effect of particle size on reactivity towards various substrates. *Catal. Today,* **181**: 26-32 (2012).

39 S T Sie, Consequences of catalyst deactivation for process design and operation. *Appl. Catal. A.,* **212**: 129-151 (2001).

40 M Signoretto, F Menegazzo, V Trevisan, F Pinna, M Manzoli, F Boccuzzi, Investigation on the Stability of Supported Gold Nanoparticles. *Catalysts,* **3**: 656-670 *(*2013).

41 A Villa, D Wang, DS Su, L Prati, Gold Sols as Catalysts for Glycerol Oxidation: The Role of Stabilizer. *Chemcatchem,* **1**: 510-514(2009).

42 A Quintanilla, VCL Butselaar-Orthlieb, C Kwakernaak, WG Sloof, MT Kreutzer, F Kapteijn, Weakly bound capping agents on gold nanoparticles in catalysis: Surface poison?. *J. Catal.*, **271**: 104-114 (2010).

43 M Manzoli, F Menegazzo, M Signoretto, D. Marchese, Biomass derived chemicals: furfural oxidative esterification to methyl-2-furoate over gold catalysts. *Catalysts,* **36**: 106-133 *(*2016).

Table 1: Catalytic performances in the 2-FA oxidative esterification (reaction at 120 °C - 6 bar O_2 – 90 min of reaction) and Au particle size of the samples.

n.d.= not determined.

	Conversion (%)	Selectivity (%)	Au mean particle size (nm)
Audp500	74	<99	3.4 ± 1.3
Ausol	>99	<99	3.0 ±1.7
Ausol300	>99	<99	n.d
Ausol500	>99	<99	4.7 ± 0.8

Table 2: Catalytic performances in the 2-FA oxidative esterification (reaction at 120 °C - 6 bar O_2 – 90 min of reaction) for previously investigated samples synthesized by dp.

	Conversion (%)	Selectivity (%)	Reference
$AuTiO_2$ WGC reference	72	73	43
$AuZrO_2$ C150	70	94	5
$AuZrO_2$ C300	82	92	6
$AuZrO_2$ C500	96	97	5
$AuTiO_2$ C300	20	90	6
$AuCeO_2$ C90C300	29	>99	43
$AuCeO_2$ C90C500	6	>99	43
$AuCeO_2$ C110C300	29	>99	43
$AuCeO_2$ C110C500	28	>99	43
$AuCeO_2$ C300C300	54	>99	8
$AuCeO_2$ C500C500	74	>99	8
$AuCeO_2$ C650C300	66	68	6

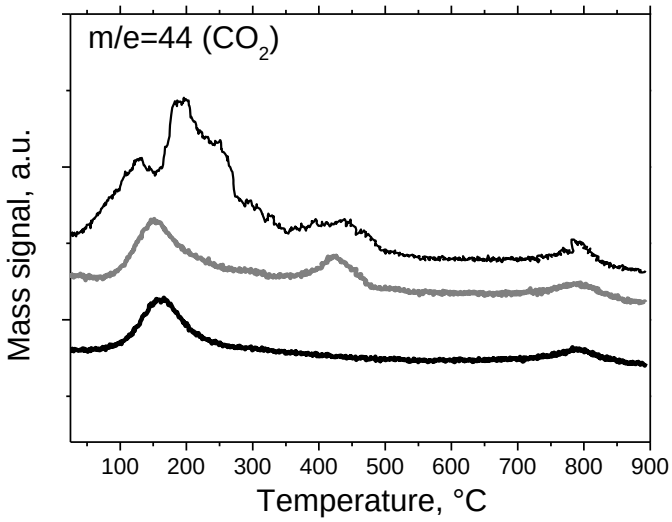

Figure 1: TPO curves for the Ausol (fine curves), Ausol300 (grey curves) and Ausol500 (bold curves) samples.

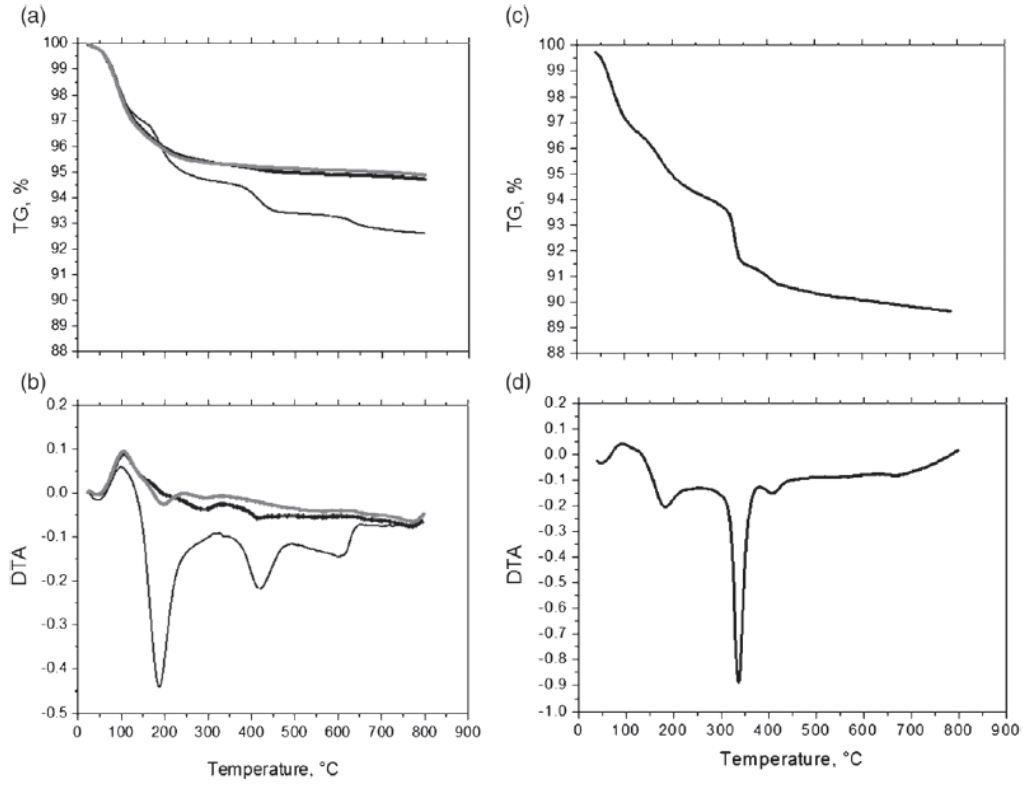

Figure 2: TG (a), DTA (b) curves for the Ausol (fine curves), Ausol300 (grey curves) and Ausol500 (bold curves) samples. TG (c) and DTA (d) curves for the used Ausol catalyst.

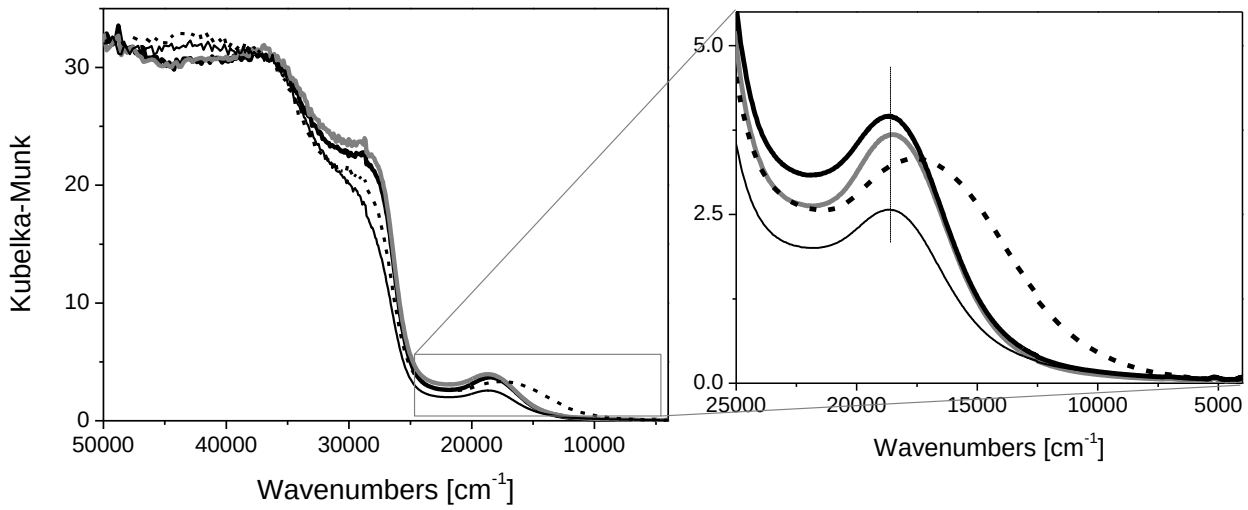

Figure 3: DRUV-Vis spectra of the as prepared Ausol (fine curve), Ausol300 (grey curve), Ausol500 (bold curve) and Audp500 (dashed curve) samples. Inset: zoom on the 25000-4000 cm^{-1} range.

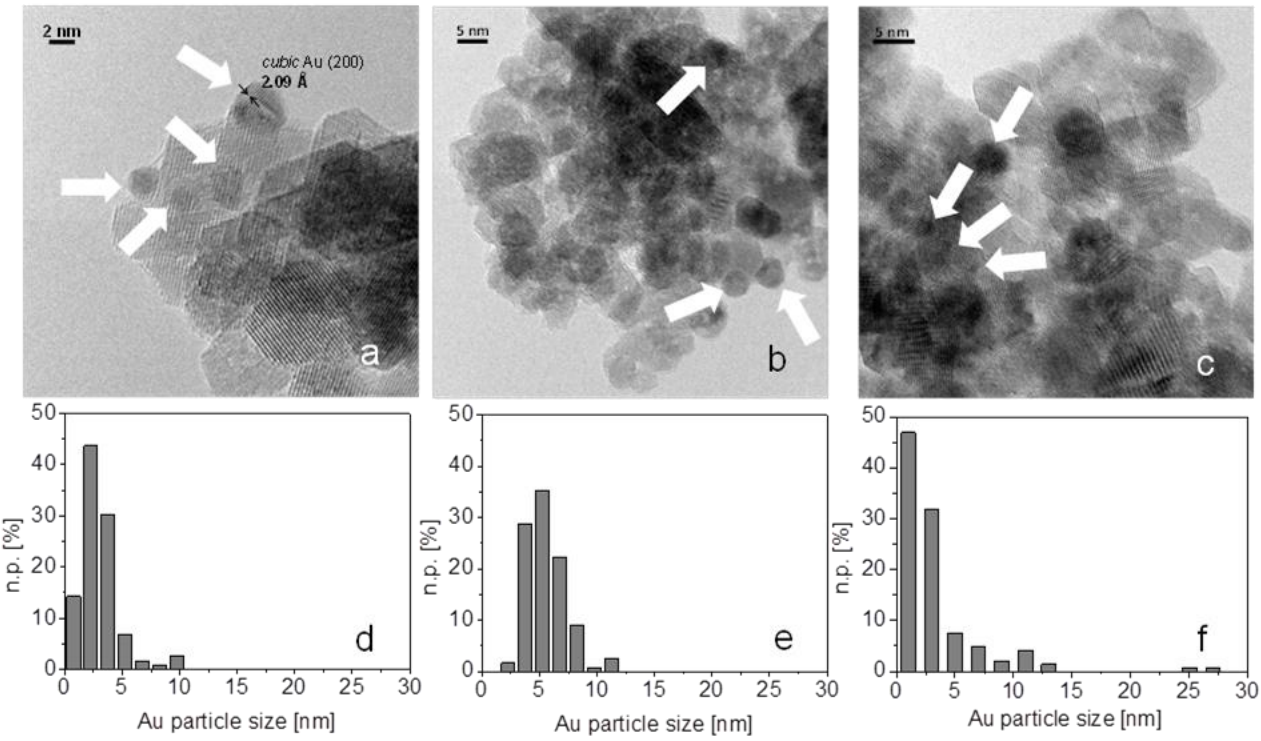

Figure 4: HRTEM images collected on Ausol (section a), Ausol500 (section b) and Audp500 (section c), where the presence of Au nanoparticles is put in evidence by arrows. Au particle size distribution of Ausol, Ausol500 and Audp500 are reported in section d, e and f, where n.p. [%]= number of counted particles of diameter d_i. Instrumental magnification: 600000X, 300000X and 400000X, respectively.

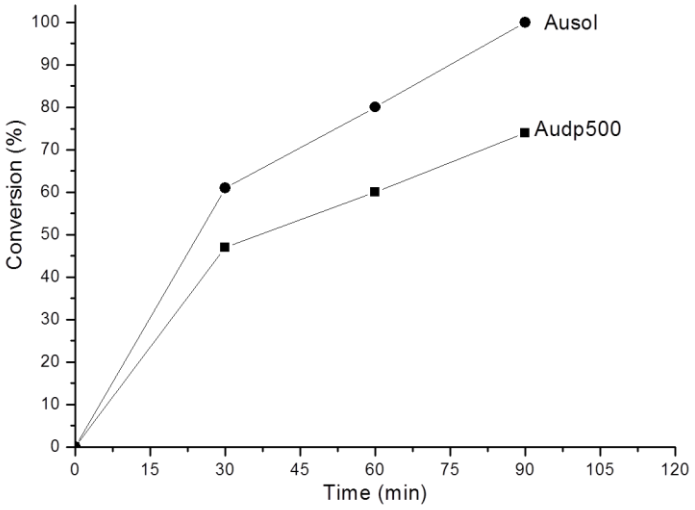

Figure 5: Catalytic performances for the samples in the 2-FA oxidative esterification (reaction at 120 °C - 6 bar O_2). Audp500 (■) and Ausol (●)

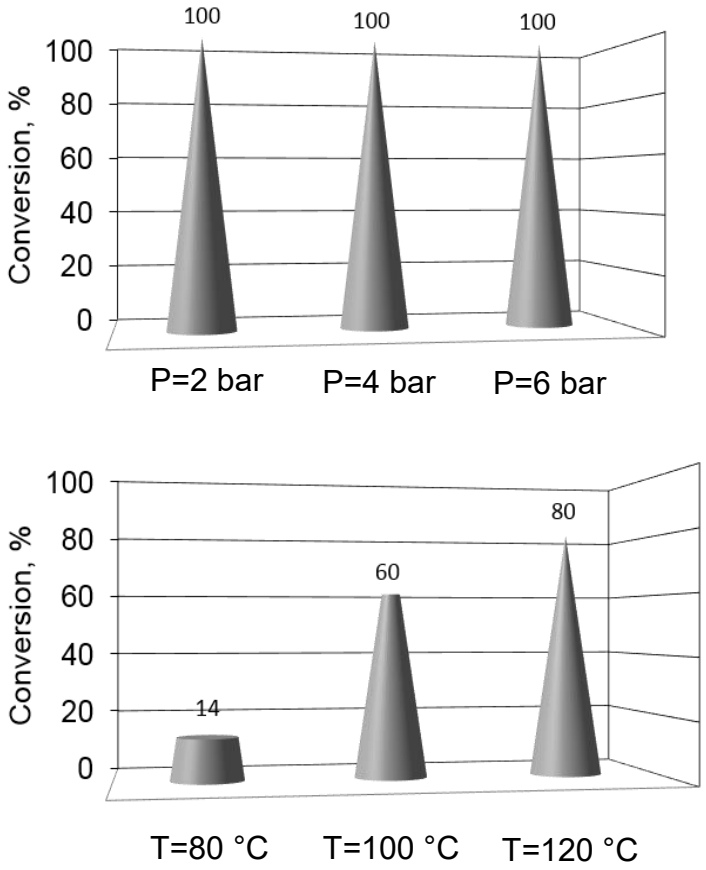

Figure 6: Effect of the pressure (at 120°C - 90 min of reaction) and effect of temperature (at 6 bar – 60 min of reaction) on the catalytic performances for the Ausol sample.

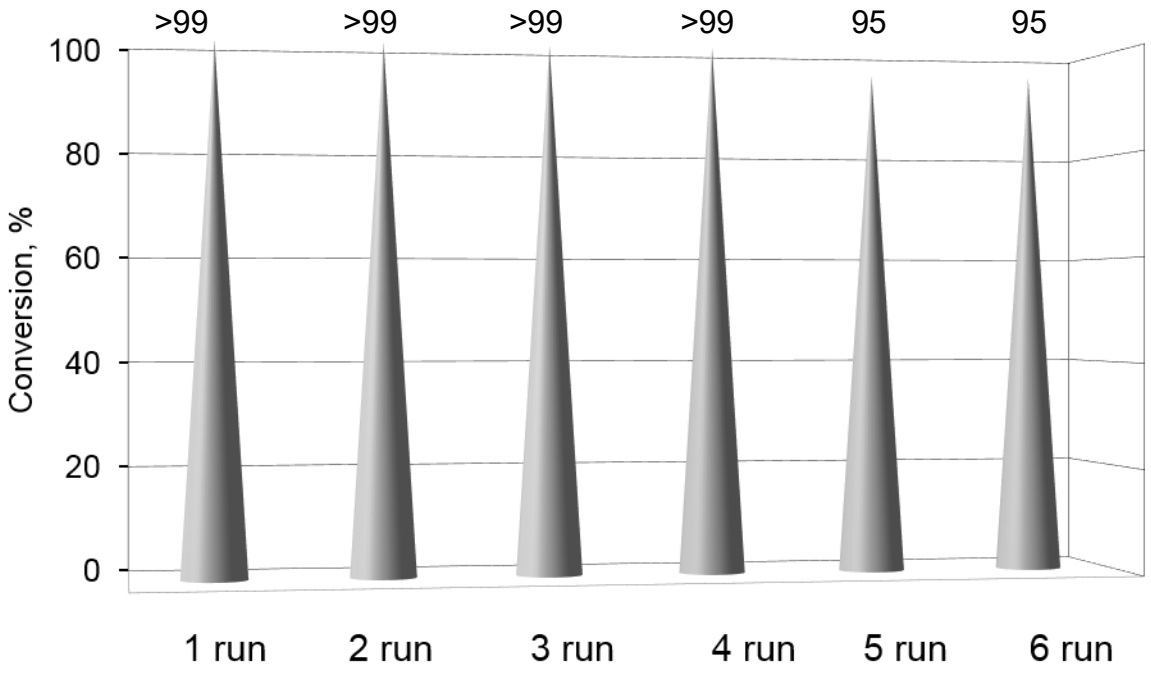

Figure 7: Recyclability of the Ausol catalyst during the 2-FA esterification tests.

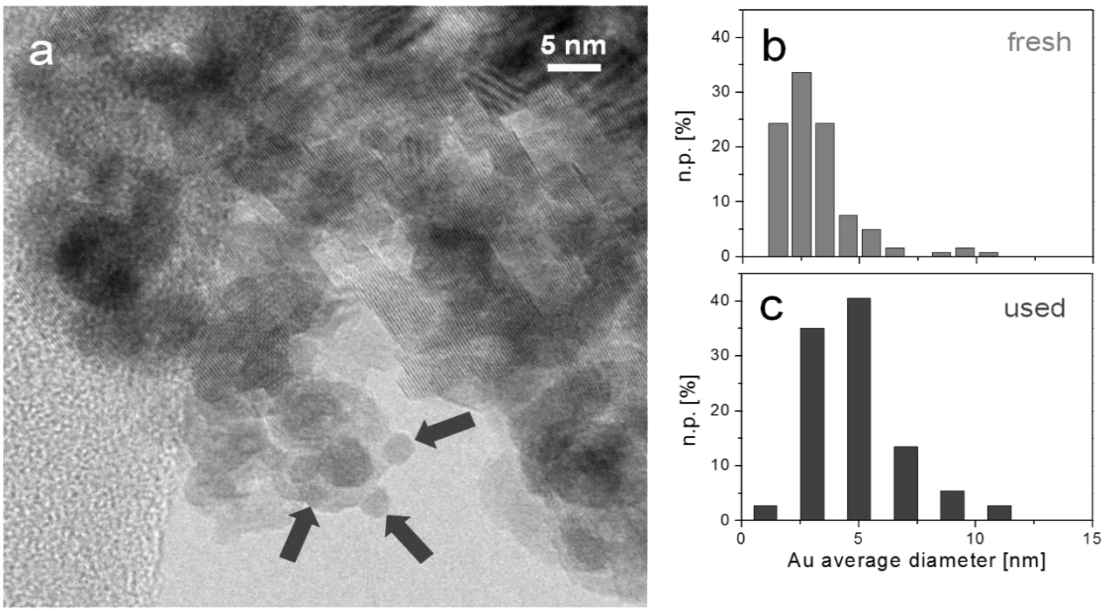

Figure 8: HRTEM image collected on Ausol used after six runs (section a), where the presence of Au nanoparticles is put in evidence by arrows. Au particle size distributions of Ausol fresh and used after six runs are compared in section b and c. Instrumental magnification: 300000X.